Polyhedron 210 (2021) 115493

Contents lists available at ScienceDirect

Polyhedron

journal homepage: www.elsevier.com/locate/poly

Synthesis of Ba(II) analogs of Ln(II)-in-(2.2.2-cryptand) and layered hexagonal net Ln(II) complexes, $[(THF)Cs(\mu\text{–}\eta^5\text{:}\eta^5\text{–}C_5H_4SiMe_3)_3Ln^{II}]_n$

Daniel N. Huh, Sierra R. Ciccone, William N.G. Moore, Joseph W. Ziller, William J. Evans *

Department of Chemistry, University of California, Irvine, CA 92697, United States

ARTICLE INFO

Dedicated to Malcolm Green, an exceptional contributor to the advancement of chemistry who led the field in so many creative ways.

Keywords:
Lanthanides
2.2.2-Cryptand
Barium
Layered hexagonal net

ABSTRACT

The Ba-in-(2.2.2-cryptand) complexes, $[Ba(2.2.2\text{-cryptand})(DMF)_2][I]_2$ and $[Ba(2.2.2\text{-cryptand})(OTf)_2]$, were synthesized from the reaction of 2.2.2-cryptand with BaI_2 and $Ba(OTf)_2$, respectively, and crystallographically characterized for comparison with lanthanide analogs. The complexes are soluble in THF, just as their Ln = Nd and Sm analogs. The reaction of a mixture of BaI_2 and KCp′ (Cp′ = $C_5H_4SiMe_3$) in THF with excess Cs metal yielded crystals of the layered complex, $[(THF)Cs(\mu\text{–}\eta^5\text{:}\eta^5\text{–}Cp')_3Ba(THF)]_n$, which was crystallographically characterized for comparison with $[(THF)Cs(\mu\text{–}\eta^5\text{:}\eta^5\text{–}Cp')_3Yb^{II}]_n$. A solvent-free analog of these complexes, $[Cs(\mu\text{–}\eta^5\text{:}\eta^5\text{–}Cp')_3Yb^{II}]_n$, is also reported such that the three structures demonstrate that the layered structure is stable to variable amounts of THF coordination, which is important in using this network as a thin film precursor.

1. Introduction

Recent studies in reductive rare-earth metal chemistry have expanded the range of crystallographically characterizable molecular complexes containing Ln(II) ions from the traditional metals Eu, Yb, Sm, Tm, Dy, and Nd, to the entire lanthanide series via reductions of Cp''_3Ln and Cp'_3Ln complexes (Cp″ = $C_5H_3(SiMe_3)_2$; Cp′ = $C_5H_4SiMe_3$) with potassium in the presence of 2.2.2-cryptand (crypt), eq 1 [1–5]. The new Ln(II) complexes of La, Ce, Pr, Gd, Tb,

Ho, Er, and Lu are highly reducing and have $4f^n5d^1$ electron configurations instead of the $4f^{n+1}$ Aufbau configurations of the traditional Ln(II) ions obtained by reduction of $4f^n$ Ln(III) precursors [2,3,6].

The generation of Ln(II) ions in the presence of crypt raised questions about the chemistry of lanthanide ions in crypt, an area that was limited to Ln(III) ions for many years [7–10]. A Eu(II)-in-crypt complex was reported in 2010 [11–13], but only recently have Sm(II) and Yb(II) complexes been found [7–16]. The synthesis of the first Nd(II)-in-crypt complex is shown in eq 2 [17]. These Ln(II)-in-crypt complexes are of interest both as novel Ln(II) species and as potential precursors to Ln(I) compounds.

To gain more information about M(II) ions in crypt, it was desirable to synthesize the analogous complexes of the alkaline-earth metal adjacent to the lanthanide series, *i.e.* Ba(II) complexes. This would allow comparisons between the lanthanides and a + 2 metal ion with no f orbital component in its electron configuration. Although Ba-in-crypt complexes have been reported in the past, many with H_2O of solvation [18–26], it was desirable to have exact analogs of the Ln(II) species for comparison and these are reported here.

Another desirable Ba(II) analog of an unusual Ln(II) complex involved the layered complex, $[(THF)Cs(\mu\text{–}\eta^5\text{:}\eta^5\text{–}Cp')_3Yb^{II}]_n$, **4**, [27] formed by reducing Cp'_3Yb with Cs in THF, eq 3. In this layered structure (see below), there is a hexagonal network of alternating Yb and Cs

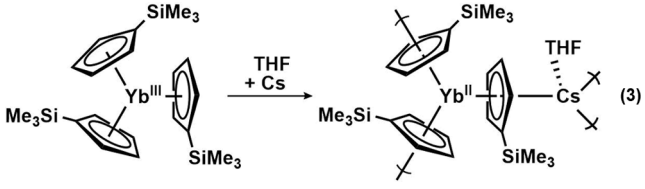

(3)

atoms, each with three bridging Cp′ ligands around each metal center. This layered complex could be used for making thin films of lanthanide networks from molecular precursors.[28] It was of interest to have a non-f element analog and hence the Ba(II) analog was investigated to see if it would form with the same structure. This gave the $[(THF)Cs(\mu\text{–}\eta^5\text{:}\eta^5\text{–}Cp')_3Ba(THF)]_n$ analog which has an additional THF molecule solvated to the Ba metal. In the course of these studies, an unsolvated complex, $[(Cs(\mu\text{–}\eta^5\text{:}\eta^5\text{–}Cp')_3Yb^{II}]$, **5**, was crystallographically

* Corresponding author.
E-mail address: wevans@uci.edu (W.J. Evans).

https://doi.org/10.1016/j.poly.2021.115493
Received 24 August 2021; Accepted 18 September 2021
Available online 24 September 2021

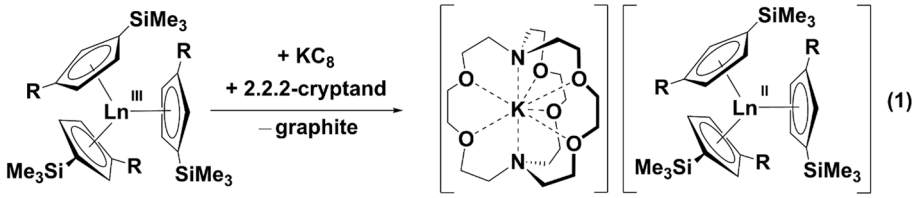

R = H; Ln = Y, La, Ce, Pr, Nd, Sm, Gd, Tb, Dy, Ho, Er, Tm, Lu
R = $SiMe_3$; Ln = La, Ce, Pr, Nd

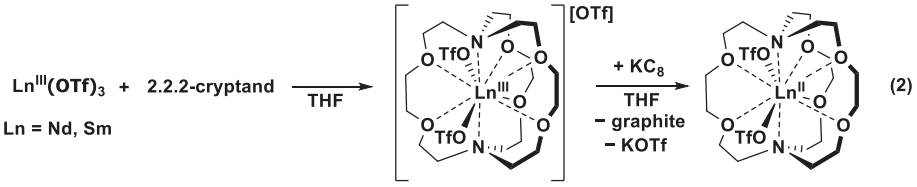

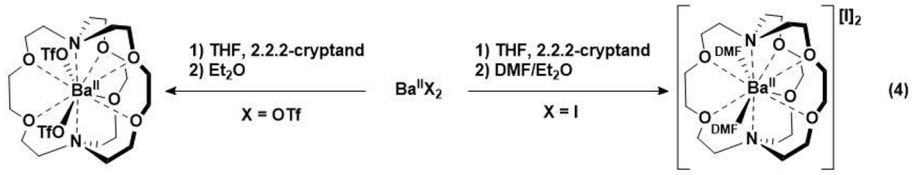

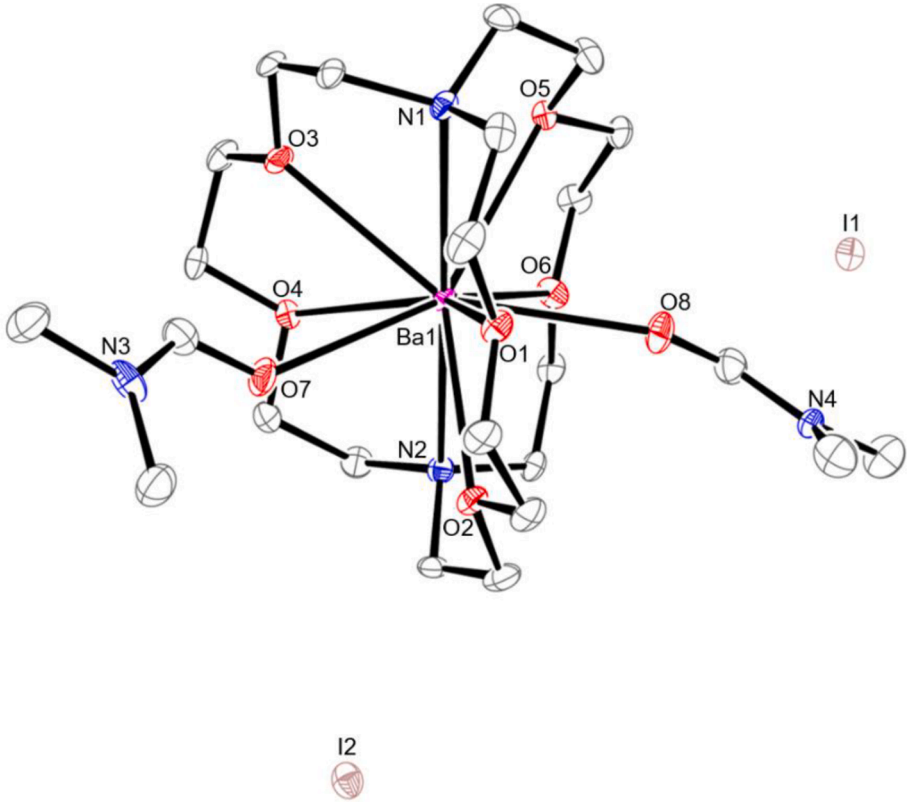

Fig. 1. X-ray crystal structure of $[Ba(crypt)(DMF)_2][I]_2$, **1**, with atomic displacement parameters drawn at the 50% probability level. Hydrogen atoms were omitted for clarity.

Table 1
Selected bond distances [Å] of Ba-in-crypt and analogous Ln-in-crypt complexes.

	M(II)–O (DMF)	M(II)–OTf	M(II)–O (crypt)	M(II)–N (crypt)
[Ba(crypt)(DMF)$_2$][I]$_2$	2.757(4)-2.790(4)	–	2.775(5)-2.894(4)	3.005(6)-3.021(6)
[Ba(crypt)(OTf)$_2$]	–	2.739(2)-2.743(2)	2.786(2)-2.850(2)	2.959(2)-2.968(2)
[Sm(crypt)(DMF)$_2$][I]$_2$	2.557(1)-2.557(1)	–	2.740(1)-2.793(1)	2.876(2)
[Sm(crypt)(OTf)$_2$]	–	2.583(2)–2.586(2)	2.703(2)-2.763(2)	2.906(2)-2.919(2)

characterized that demonstrates the flexibility of the layered structure to solvation.

2. Results and discussion

Encapsulation of Ba(II). Syntheses of Ba(II)-in-crypt complexes (crypt = 2.2.2-cryptand) were achieved by addition of BaI_2 and $Ba(OTf)_2$ to crypt, eq 4. Addition of a suspension of BaI_2

in THF to a THF solution of crypt generated a colorless precipitate that was soluble in DMF. Single-crystals suitable for X-ray diffraction were obtained from DMF/Et_2O yielding the complex [Ba(crypt)(DMF)$_2$][I]$_2$, **1**, Fig. 1. Complex **1** is not isomorphous with [Ln(crypt)(DMF)$_2$][I]$_2$ (Ln = Sm, Eu) [14], but the structure is similar. Bond distances are compared in Table 1.

Addition of a THF solution of $Ba(OTf)_2$ to a THF solution of crypt generated a colorless solution rather than a precipitate. Crystallization from THF/Et_2O generated [Ba(crypt)(OTf)$_2$], **2**, which also was characterized by X-ray diffraction, Fig. 2, eq 4. Complex **2** is isomorphous with the Nd and Sm complexes, [Ln(crypt)(OTf)$_2$], which are also soluble in THF. Interestingly, although triflate is a weakly coordinating anion, in the case of **2**, it binds more strongly than THF.

Ba(II)-in-Crypt Structural Data. The Ba(II) centers in **1** and **2** both have a 10-coordinate geometry generated by the eight donor atoms of crypt and two additional inner-sphere ligands of DMF or OTf, respectively. In the case of **1**, there are also two outer-sphere iodides present. The coordination geometry around Ba can be described as a tetra-capped trigonal prism with crypt N donors capping the triangular faces and the inner-sphere OTf or DMF ligands capping two of the rectangular faces.

Structural data on **1**, **2**, and their Sm(II) analogs are summarized in Table 1. In **1**, the 2.757(4)-2.790(4) Å Ba–O(DMF) distances of the neutral DMF overlap with the 2.775(5)-2.894(4) Å Ba–O(crypt) range of distances and the 3.005(6)-3.021(6) Å Ba–N(crypt) distances are the longest of all. In **2**, the 2.739(2)-2.743(2) Å Ba–O(OTf) distances of the anionic triflate are shorter than the 2.786(2)-2.850(2) Ba–O(crypt). As in **1**, the 2.959(2)-2.968(2) Ba–N(crypt) distances are the longest. The Ba–crypt distances in **1** and **2** are similar to the 2.698(9)-3.03(2) Å Ba–O (crypt) and 2.90(1)-3.025(2) Å Ba–N(crypt) distances for previously reported Ba-in-crypt complexes (See Table S9 and S10 for a full compilation).

The Sm and Eu analogs of **1** and the Nd and Sm analogs of **2** have metrical parameters that vary as their Shannon ionic radii vary (Tables S9 and S10), so comparison with the Ba complexes can be made with just one lanthanide. Sm(II) is used since there are analogs to both **1** and **2**. Since the Shannon ionic radius of Ba(II) is about 0.15 Å larger

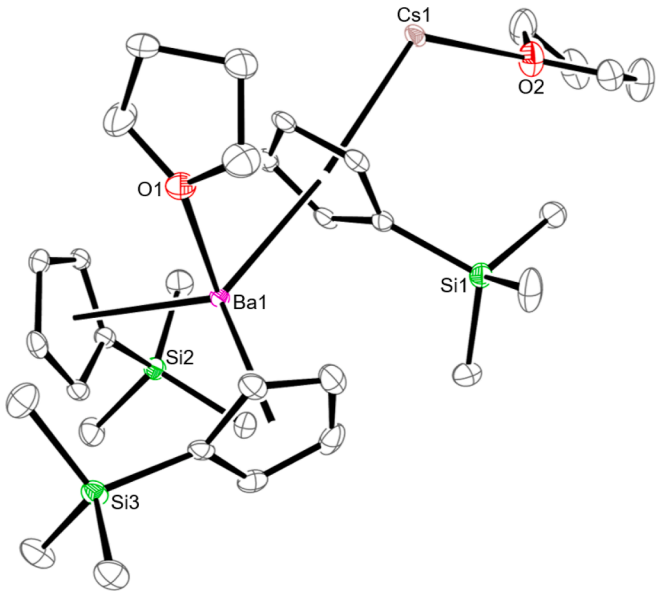

Fig. 3. X-ray crystal structure of [(THF)Cs(μ–η^5:η^5–Cp′)$_3$Ba(THF)]$_n$, with thermal ellipsoids drawn at the 50% probability level. Disorder of a coordinated THF and hydrogen atoms were omitted for clarity.

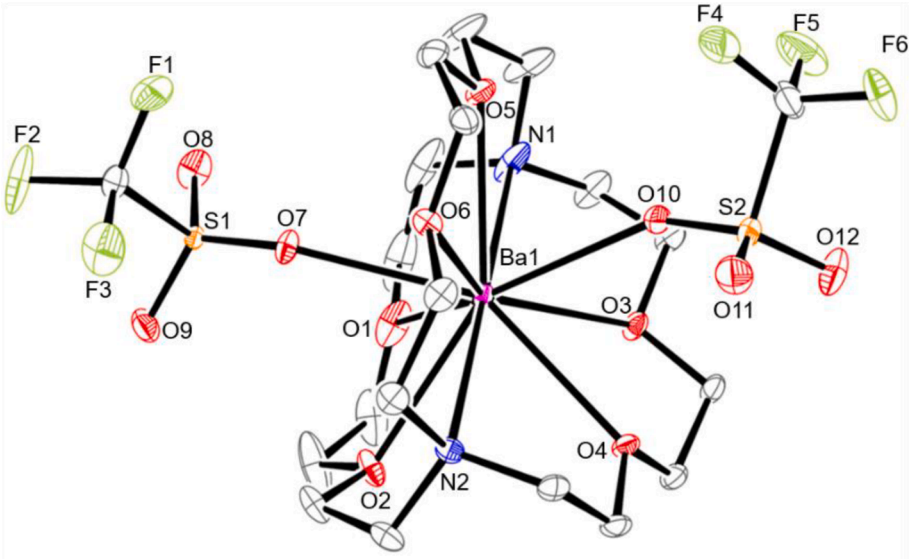

Fig. 2. X-ray crystal structure representation of [Ba(crypt)(OTf)$_2$], **2**, with atomic displacement parameters drawn at the 50% probability level. Disorder of a coordinated OTf and hydrogen atoms were omitted for clarity.

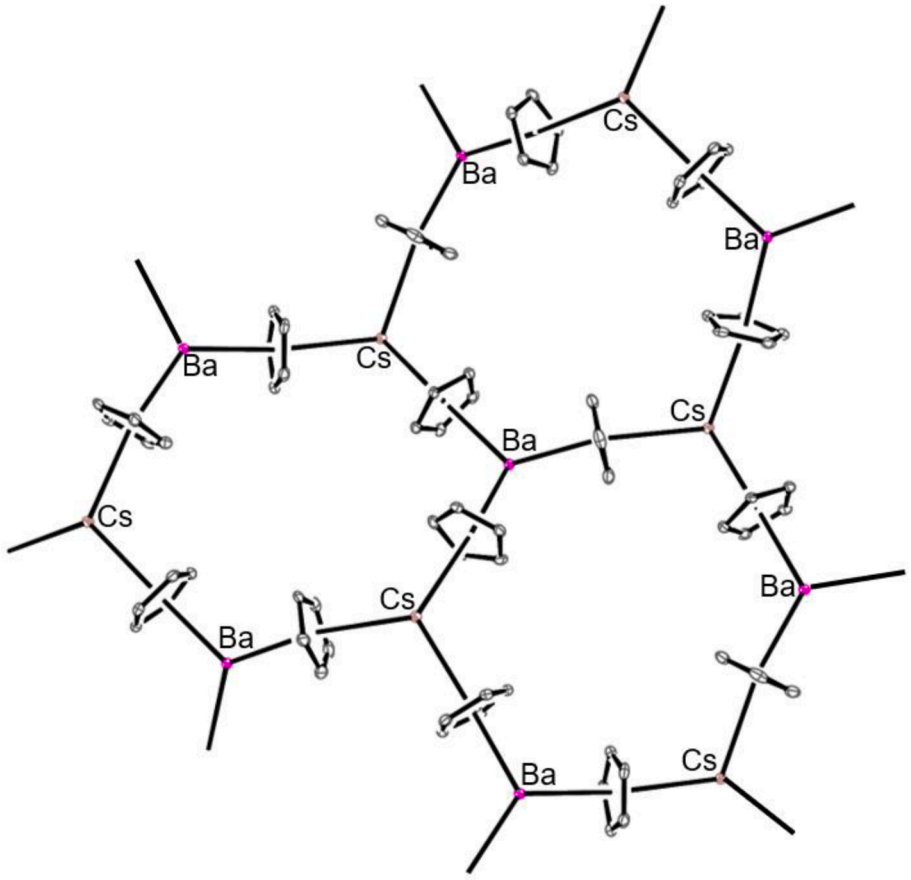

Fig. 4. Top view of the extended structure of $[(THF)Cs(\mu\text{–}\eta^5\text{:}\eta^5\text{–}Cp')_3Ba(THF)]_n$, **3**, where Cs = gray, Ba = magenta. The $SiMe_3$ substituent of Cp′ ligands and THF molecules were removed for clarity.

than that of Sm(II) [29], it is reasonable that the Ba-O(DMF) and Ba-O (OTf) distances are about 0.20 and 0.16 Å longer than the Sm analogs. The ranges of the Ba-O(crypt) and Ba-N(crypt) distances are, however, closer to those of Sm. This attests to the flexibility of the crypt ligand to adjust to metals of different size.

Synthesis of a Layered Ba(II) Complex. $[(THF)Cs(\mu\text{–}\eta^5\text{:}\eta^5\text{–}Cp')_3Ba(THF)]_n$, **3**, was synthesized directly from BaI_2, KCp′, and excess Cs metal. A THF suspension of BaI_2 was added to a THF solution of two equivalents of KCp′, stirred overnight, and then filtered into a vial containing a Cs metal smear. The colorless mixture was stored in a −35 °C freezer overnight and subsequently filtered into a layer of Et_2O. Colorless single crystals obtained the next day were structurally characterized as $[(THF)Cs(\mu\text{–}\eta^5\text{:}\eta^5\text{–}Cp')_3Ba(THF)]_n$, **3**, shown in eq 5 and with the repeat unit shown in Fig. 3. Since no net reduction by Cs was observed with barium, in contrast to eq 3, the reaction constitutes an unusual method to introduce a cesium cation to this complex.

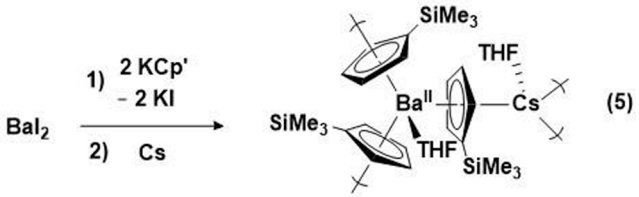

(5)

The structure of $[(THF)Cs(\mu\text{–}\eta^5\text{:}\eta^5\text{–}Cp')_3Ba(THF)]_n$, **3**, is very similar to that of $[(THF)Cs(\mu\text{–}\eta^5\text{:}\eta^5\text{–}Cp')_3Yb^{II}]$, **4** [27], except that in **3** both Cs(I) and the Ba(II) ion have coordinated THF molecules. Both structures are comprised of layers of hexagonal nets containing three Cs(I) ions and three M(II) ions, Figs. 4 and 5.

Examination of the variable temperature ^1H NMR spectra of the Yb (II) complex $[(THF)Cs(\mu\text{–}\eta^5\text{:}\eta^5\text{–}Cp')_3Yb^{II}]_n$, **4**, in THF suggested that an equilibrium exists between **4** and $Cp'_2Yb^{II}(THF)_2$ and CsCp′ (see SI for NMR data). When **4** was recrystallized from acetonitrile/diethyl ether, a solvent-free analog of the mono-THF **4** and bis-THF **3** complexes was formed: $[Cs(\mu\text{–}\eta^5\text{:}\eta^5\text{–}Cp')_3Yb^{II}]_n$, **5**, Fig. 6. This demonstrated that the hexagonal network layered structure could be accessed using solvent-based crystallization methods in three levels of solvation and that neither acetonitrile nor diethyl ether readily coordinated in the THF locations of **3** and **4**.

Metrical data on **3**, **4** and **5** are presented in Table 3. The Yb-Cp'_{cent} (Cp'_{cent} = Cp′ ring centroid) distances in **4** and **5** are similar as expected for the similar coordination environments for Yb in each. The Cs–Cp'_{cent} distances in **4** and **5** overlap, but the higher coordinated **3** has some longer distances as expected for a higher coordinate metal atom. The Ba–Cp'_{cent} distances are about 0.35 Å longer than the Yb–Cp'_{cent} distances in **4** and **5** which is a difference close to the 0.28 Å larger size of Ba(II) and the 0.05 Å increase in bond distances that accompanies an increase by one of coordination number according to Shannon radii [29].

To determine how the degree of THF solvation affected the planarity of the hexagonal rings, the root-mean-square deviations (RMSD) of the six metal vertices from the mean plane of their positions for **3**, **4** and **5** were calculated. The ω_{hex} = 0.697 Å value for the bis-THF **3** is remarkably similar to the ω_{hex} = 0.671 Å value for mono-THF **4**. However, the ω_{hex} = 0.500 Å value for THF-free **5** is much smaller, indicating a more planar structure.

To further assess the effect of THF on the corrugated nature of these structures, the dihedral angles between adjacent planes of six metal atom hexagons were measured. The solvent-free Yb structure **5** yields a

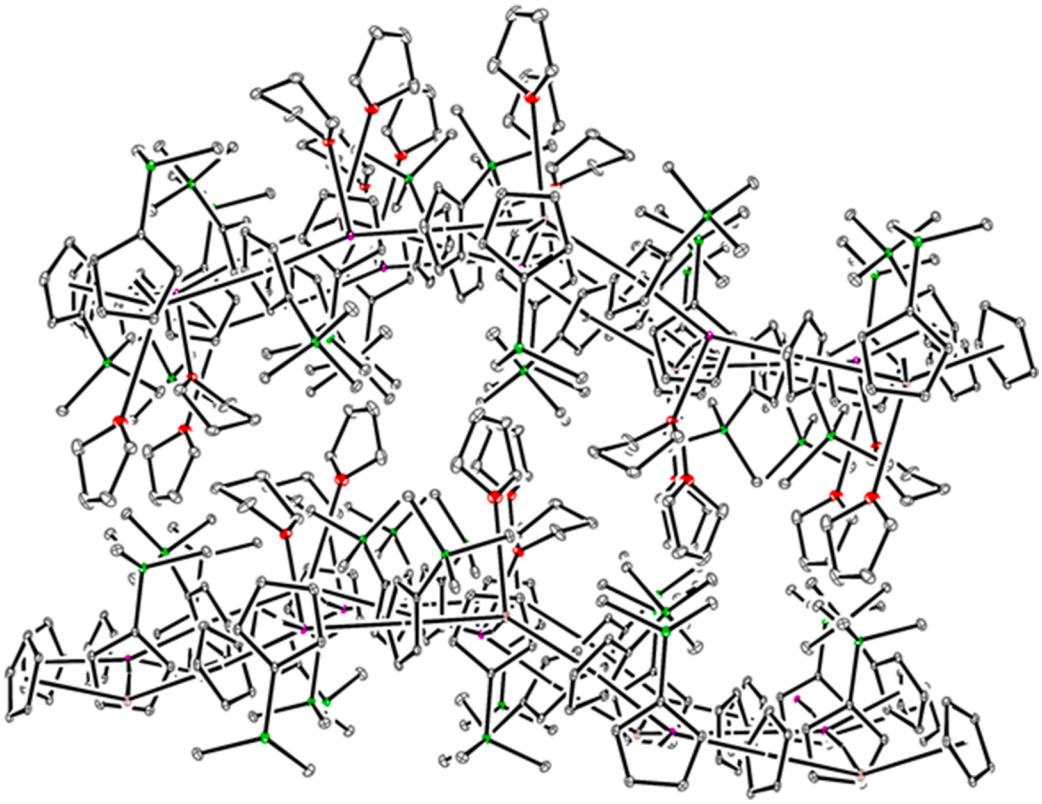

Fig. 5. Side view of the extended structure of [(THF)Cs(μ–η^5:η^5–Cp′)$_3$Ba(THF)]$_n$, **3**, where Cs = gray, Ba = magenta.

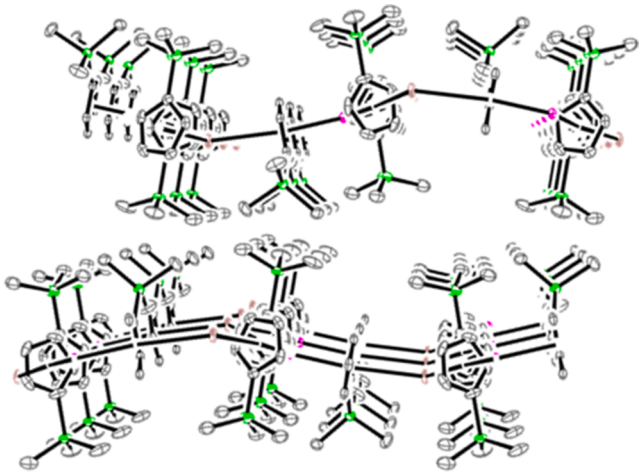

Fig. 6. Side view of the extended structure of [Cs(μ–η^5:η^5–Cp′)$_3$Yb]$_n$, **5**, where Cs = brown and Yb = magenta.

Table 3
Summary of bond length (Å) ranges of select [Cs(μ–η^5:η^5–Cp′)$_3$M]$_n$ oligomeric complexes, **3**–**5**, RMSD calculations (ω_{hex}, Å) for Cs(I)/M(II) hexagons, and dihedral angles.

	M(II)–Cp′$_{cent}$	Cs(I)–Cp′$_{cent}$	ω_{hex} (A)	Dihedral Angle
[(THF)Cs(u–n^5:n ^{5}–Cp′)$_3$Ba(THF)]n **3**	2.852–2.875	3.202–3.244	0.697	29.70
[(THF)Cs(u–n^5:n ^{5}–Cp′)$_3$Yb]$_n$ **4**	2.503–2.510	3.159–3.268	0.671	20.26
[Cs(u–n^5:n ^{5}–Cp′)$_3$Yb]$_n$ **5**	2.510–2.523	3.141–3.183	0.500	12.89

dihedral angle of 12.89°, and the mono-THF Yb structure **4** yields a dihedral angle of 20.26°, consistent with the difference seen in the RMSD value. Interestingly, complex **3** shows a marked difference with respect to **4**, in this case, with a greater dihedral angle of 29.70°. Together, these three structures demonstrate that the hexagonal layers can be reliably replicated with zero, one, and two coordinated THF molecules in the repeat units.

The structures of **3**–**5** can also be compared with [Na(μ–η^5:η^5–C$_5$H$_5$)$_3$Yb^{II}]$_n$, **6** [30], which can be generated by reduction of (C$_5$H$_5$)$_3$Yb with sodium naphthalenide or by reaction of (C$_5$H$_5$)$_2$Yb with Na(C$_5$H$_5$). Complex **6** is an analog of **5**, but with Na in place of Cs and unsubstituted C$_5$H$_5$ instead of C$_5$H$_4$SiMe$_3$. Complex **6** differs from **3 to 5** in that crystals were obtained by sublimation at 400 °C. Although **6** has an extended structure, it is a 3-dimensional structure and does not exist in layers. The difference in structure could be due to the different size of the alkali metal, the different method of crystallization, or the fact that **6** does not have the SiMe$_3$ groups that are found between the layers in **3**–**5**. All of these differences provide bases upon which to test crystal engineering in this system in the future.

3. Conclusion

Barium analogs of Ln(II)-in-crypt and layered Ln(II) metallocene systems were synthesized and crystallographically characterized to compare a + 2 ion without energetically accessible f or d orbitals to Ln (II) ions in the same coordination environments. Direct analogs of [Ln (crypt)(DMF)$_2$][I]$_2$ and [Ln(crypt)(OTf)$_2$] were obtainable with Ba that demonstrate the flexibility of the 2.2.2-cryptand ligand. Isolation of [(THF)Cs(μ–η^5:η^5–Cp′)$_3$Ba(THF)]$_n$, demonstrated that the layered structure of hexagonal nets of M(II)/Cs compounds composed of [Cs (μ–η^5:η^5–Cp′)$_3$M]$_n$ units, can accommodate THF on both the Cs and the M(II) ion. The isolation of [Cs(μ–η^5:η^5–Cp′)$_3$Yb]$_n$ revealed that these layered compounds can maintain their structural integrity even in the absence of solvent. This is valuable information for future studies using

these compounds as synthetically manipulatable molecular precursors to thin films with emergent properties.

4. Experimental

All syntheses and manipulations described below were conducted under Ar with rigorous exclusion of air and water using glovebox, Schlenk-line, and high-vacuum-line techniques. BaI_2 and $Ba(OTf)_2$ were purchased from Strem and used as purchased. 2.2.2-Cryptand (4,7,13,16,21,24-hexaoxa-1,10-diazabicyclo[8.8.8]hexacosane, Aldrich) was placed under vacuum for 12 h (1×10^{-3}Torr) before use. KCp′ [31] and $[(THF)Cs(\mu\text{–}\eta^5\text{:}\eta^5\text{–}Cp')_3Yb]_n$ [27] were prepared according to previously published literature. Solvents were sparged with UHP Ar and dried over columns containing Q-5 and molecular sieves. ^{1}H (500 MHz) NMR and ^{133}Cs (65 MHz) NMR spectra were obtained on a Bruker GN500 MHz spectrometer at 25 °C in THF-d_8 or C_6D_6, unless otherwise stated. IR samples were collected on an Agilent Cary 630 equipped with a diamond ATR attachment. Elemental analyses were performed on a PerkinElmer series II 2400 CHNS analyzer.

$[Ba(crypt)(DMF)_2][I]_2$, 1. In an argon-filled glovebox, a suspension of BaI_2 (50 mg, 0.128 mmol) in THF (2 mL) was added to a stirring colorless solution of 2.2.2-cryptand (48 mg, 0.128 mmol). A colorless precipitate immediately formed and the mixture was stirred overnight. The solvent was removed *in vacuo* yielding a colorless solid. This was redissolved in DMF, layered into Et_2O, and placed into a –35 °C freezer. After 1 d, X-ray quality colorless crystals were isolated (38 mg, 68 %). IR $\tilde{\upsilon}$, cm^{-1}: 2865 m, 2206w, 2063w, 1620 s, 1441w, 1400 m, 1353 m, 1296 m, 1253 m, 1155w, 1067 s, 948 s, 825 m, 743 m. ^{1}H NMR δ, ppm (500 MHz, DMF-d_7): 3.77 (t, 12H), 3.73 (s, 12H), 2.79 (t, 12H). Anal. Calcd. for the desolvated $[Ba(crypt)][I]_2$, $C_{18}H_{36}BaI_2N_2O_6$: C, 28.16; H, 4.73; N, 3.65. Found: C, 28.18; H, 4.48; N, 3.29.

$[Ba(crypt)(OTf)_2]$, 2. In an argon-filled glovebox, a colorless solution of $Ba(OTf)_2$ (50 mg, 0.114 mmol) in THF (2 mL) was added to a stirring colorless solution of 2.2.2-cryptand (43 mg, 0.114 mmol). This colorless solution was stirred overnight. The colorless solution was filtered and then layered with Et_2O and placed in a –35 °C freezer. After 1 d, X-ray quality colorless crystals were isolated (61 mg, 66%). IR $\tilde{\upsilon}$, cm^{-1}: 2877w, 1480w, 1446w, 1356w, 1246 s, 1153 m, 1087 s, 1029 s, 949 m, 828w, 755w. ^{1}H NMR δ, ppm (600 MHz, THF-d_8): 3.83 (s, 12H), 3.76 (s, 12H), 2.72 (s, 12H): ^{19}F[^{1}H] NMR δ, ppm (564 MHz, THF-d_8): −77.21 (OTf). Anal. Calcd. for $[Ba(crypt)(OTf)_2]$, $C_{20}H_{36}N_2O_{12}F_6S_2Ba$: C, 29.59; H, 4.47; N, 3.45. Found: C, 29.19; H, 4.53; N, 3.30.

$[(THF)Cs(\mu\text{–}\eta^5\text{:}\eta^5\text{–}Cp')_3Ba(THF)]_n$, 3. In an argon-filled glovebox, a suspension of BaI_2 (50 mg, 0.13 mmol) in THF (2 mL) was added to a stirring colorless solution of KCp′ (45 mg, 0.26 mmol) in THF, and the mixture was stirred overnight. The resulting colorless solution was filtered into a vial containing a Cs metal smear and placed into a –35 °C freezer overnight. The colorless mixture was then filtered into a vial containing Et_2O and placed again into a –35 °C freezer. After 1 d, X-ray quality colorless crystals of **3** were isolated (36 mg, 34%). IR $\tilde{\upsilon}$, cm^{-1}: 3072 m, 2948w, 2870w, 1580w, 1438w, 1352w, 1242 s, 1181w, 1038 m, 1008 s, 902w, 829 s, 725 s. ^{1}H NMR δ, ppm (500 MHz, THF-d_8): 5.58 (s, 12H), 0.09 (s, 27H). ^{133}Cs NMR δ, ppm (65 MHz, THF-d_8): −216.30 (s). Anal. Calcd. for $[(THF)Cs(\mu\text{–}\eta^5\text{:}\eta^5\text{–}Cp')_3Ba(THF)]_n$, $C_{32}H_{55}BaCsO_2Si_3$: C, 46.52; H, 6.71. Found: C, 36.70; H, 4.27. The incomplete combustion observed with this sample sometimes occurs with silicon-containing complexes.[32-35] The observed CH ratio for this complex was $C_{32}H_{45}$.

$[Cs(\mu\text{–}\eta^5\text{:}\eta^5\text{–}Cp')_3Yb]_n$, 5. Crystals of $[(THF)Cs(\mu\text{–}\eta^5\text{:}\eta^5\text{–}Cp')_3Yb]_n$ (50 mg, 0.06 mmol) were evacuated at room temperature for 30 min and subsequently dissolved in cold acetonitrile. Light blue crystals of **5** (21 mg, 46%) were grown from slow vapor diffusion of Et_2O into the acetonitrile solution at − 35 °C over the course of 1 day. IR $\tilde{\upsilon}$, cm^{-1}: 3073w, 2947w, 2893w, 1438w, 1400w, 1353w, 1306w, 1242 m, 1176 m, 1035 m, 903 m, 824 s, 742 s, 680 m. UV–vis λ_{max}, nm (ε, M^{-1} cm^{-1}): 375 (950) and 610 (300). ^{1}H NMR δ, ppm (500 MHz, CD_3CN): 5.91 (s, 6H) , 5.79 (s, 6H), 0.12 (s, 27H). ^{133}Cs NMR δ, ppm (65 MHz, CD_3CN): −106.55 (s). Anal. Calcd. for $[Cs(\mu\text{–}\eta^5\text{:}\eta^5\text{–}Cp')_3Yb]_n$, $C_{24}H_{39}CsSi_3Yb$: C, 40.16; H, 5.48. Found: C, 38.57; H, 5.17. The incomplete combustion observed with this sample sometimes occurs with silicon-containing complexes [31–36], but the observed CH ratio, $C_{24}H_{38}$, is close to the calculated.

CRediT authorship contribution statement

Daniel N. Huh: Conceptualization, Methodology, Investigation, Visualization. **Sierra R. Ciccone:** Investigation, Visualization. **William N.G. Moore:** Investigation, Visualization. **Joseph W. Ziller:** Formal analysis. **William J. Evans:** Visualization, Supervision, Project administration, Funding acquisition.

Declaration of Competing Interest

The authors declare that they have no known competing financial interests or personal relationships that could have appeared to influence the work reported in this paper.

Acknowledgements

For this research, we thank the U.S. National Science Foundation (CHE-1855328 to W.J.E.). We also thank Chen Sun for assistance with X-ray crystallography.

Appendix A. Supplementary data

CCDC 2104995–2104997 and CCDC 2104658 contain the supplementary crystallographic data for $[Ba(crypt)(DMF)_2][I]_2$, $[Ba(crypt)(OTf)_2]$, $[(THF)Cs(\mu\text{–}\eta^5\text{:}\eta^5\text{–}Cp')_3Ba(THF)]_n$, and $[Cs(\mu\text{–}\eta^5\text{:}\eta^5\text{–}Cp')_3Yb]_n$. These data can be obtained free of charge via http://www.ccdc.cam.ac.uk/conts/retrieving.html, or from the Cambridge Crystallographic Data Centre, 12 Union Road, Cambridge CB2 1EZ, UK; fax: (+44) 1223–336-033; or e-mail: deposit@ccdc.cam.ac.uk.

Supplementary data to this article can be found online at https://doi.org/10.1016/j.poly.2021.115493.

References

[1] P.B. Hitchcock, M.F. Lappert, L. Maron, A.V. Protchenko, Lanthanum does form stable molecular compounds in the +2 oxidation state, Angew. Chem. Int. Ed. 47 (2008) 1488–1491.
[2] M.R. MacDonald, J.E. Bates, J.W. Ziller, F. Furche, W.J. Evans, Completing the series of +2 ions for the lanthanide elements: synthesis of molecular complexes of Pr^{2+}, Gd^{2+}, Tb^{2+}, and Lu^{2+}, J. Am. Chem. Soc. 135 (2013) 9857–9868.
[3] M.R. MacDonald, J.E. Bates, M.E. Fieser, J.W. Ziller, F. Furche, W.J. Evans, Expanding rare-earth oxidation state chemistry to molecular complexes of holmium(II) and erbium(II), J. Am. Chem. Soc. 134 (2012) 8420–8423.
[4] M.R. MacDonald, J.W. Ziller, W.J. Evans, Synthesis of a crystalline molecular complex of Y^{2+}, $[(18\text{-crown-6})K][(C_5H_4SiMe_3)_3Y]$, J. Am. Chem. Soc. 133 (2011) 15914–15917.
[5] C.T. Palumbo, L.E. Darago, C.J. Windorff, J.W. Ziller, W.J. Evans, Trimethylsilyl versus Bis(trimethylsilyl) Substitution in Tris(cyclopentadienyl) Complexes of La, Ce, and Pr: Comparison of Structure, Magnetic Properties, and Reactivity, Organometallics 37 (2018) 900–905.
[6] M.E. Fieser, M.R. MacDonald, B.T. Krull, J.E. Bates, J.W. Ziller, F. Furche, W. J. Evans, Structural, spectroscopic, and theoretical comparison of traditional vs recently discovered Ln^{2+} ions in the $[K(2.2.2\text{-cryptand})][(C_5H_4SiMe_3)_3Ln]$ complexes: the variable nature of Dy^{2+} and Nd^{2+}, J. Am. Chem. Soc. 137 (1) (2015) 369–382.
[7] J.H. Burns, Crystal and Molecular Structure of a Cryptate Complex of Samarium: $C_{18}H_{36}O_6N_2Sm_2(NO_3)_6 \cdot H_2O$, Inorg. Chem. 18 (1979).
[8] F.B. Benetollo, G.A. Cassol, G. De Paoli, J. Legendziewicz, Coordination Chemistry of Lanthanides with Cryptands. An X-ray and Spectroscopic Study of the Complex $Nd_2(NO_3)_6[C_{18}H_{36}O_6N_2]\cdot H_2O$, Inorg. Chem. Acta 110 (1985) 7–13.
[9] G.L. Yang, S. Jin, J. Zhongsheng, Coordination Chemistry and Structure Characterization $C_{18}H_{36}O_6N_2Eu_2(NO_3)_6\cdot H_2O$, Inorg. Chem. Acta 131 (1987) 125–128.
[10] J.J. Mao, Z.,, Synthesis and structure characterization of lanthanum [2,2,2] cryptates, $[LaCl[2,2,2](H_2O)]Cl_2\cdot H_2O$ and $[La(CF_3SO_3)[2,2,2](DMF)](CF_3SO_3)_2$, Polyhedron 13 (1994) 319–323.

[11] N.D. Gamage, Y. Mei, J. Garcia, M.J. Allen, Oxidatively stable, aqueous europium (II) complexes through steric and electronic manipulation of cryptand coordination chemistry, Angew. Chem. Int. Ed. 49 (2010) 8923–8925.
[12] C.U. Lenora, F. Carniato, Y. Shen, Z. Latif, E.M. Haacke, P.D. Martin, M. Botta, M. J. Allen, Structural Features of Europium(II)-Containing Cryptates That Influence Relaxivity, Chem. 23 (2017) 15404–15414.
[13] L.A. Ekanger, L.A. Polin, Y. Shen, E.M. Haacke, P.D. Martin, M.J. Allen, A Eu(II)-Containing Cryptate as a Redox Sensor in Magnetic Resonance Imaging of Living Tissue, Angew. Chem. Int. Ed. 54 (2015) 14398–14401.
[14] D.N. Huh, J.W. Ziller, W.J. Evans, Facile Encapsulation of Ln(II) Ions into Cryptate Complexes from $LnI_2(THF)_2$ Precursors (Ln = Sm, Eu, Yb), Inorg. Chem. 58 (2019) 9613–9617.
[15] D.N. Huh, C.M. Kotyk, M. Gembicky, A.L. Rheingold, J.W. Ziller, W.J. Evans, Synthesis of rare-earth-metal-in-cryptand dications, [Ln(2.2.2-cryptand)]2+, from Sm2+, Eu2+, and Yb2+ silyl metallocenes (C5H4SiMe3)2Ln(THF)2, Chem. Commun. 53 (2017) 8664–8666.
[16] T.C. Jenks, A.N.W. Kuda-Wedagedara, M.D. Bailey, C.L. Ward, M.J. Allen, Spectroscopic and Electrochemical Trends in Divalent Lanthanides through Modulation of Coordination Environment, Inorg. Chem. 59 (4) (2020) 2613–2620.
[17] D.N. Huh, S.R. Ciccone, S. Bekoe, S. Roy, J.W. Ziller, F. Furche, W.J. Evans, Synthesis of Ln(II)-in-Cryptand Complexes by Chemical Reduction of Ln(III)-in-Cryptand Precursors: Isolation of a Nd(II)-in-Cryptand Complex, Angew. Chem. Int. Ed. 59 (37) (2020) 16141–16146.
[18] D.B. Fox, R. Liantonio, P. Metrangolo, T. Pilati, G. Resnati, Perfluorocarbon-hydrocarbons self-assembly: halogen bonding mediated intermolecular recognition, J. Fluorine Chem. 125 (2) (2004) 271–281.
[19] P. Metrangolo, T. Pilati, G. Resnati, in: Handbook of Fluorous Chemistry, Wiley, 2004, pp. 507–520, https://doi.org/10.1002/3527603905.ch12c.
[20] B. Masci, P. Thuéry, Complex-within-complex assemblages from {M([2.2.2] cryptand)(H2O)2}2+ (M = Sr, Ba) and {UO2(p-tert-butyl[3.1.3.1] homooxacalixarene – 4H)}2−, CrystEngComm 8 (10) (2006) 764–772.
[21] B. Metz, D. Moras, R. Weiss, Coordination des cations alcalino-terreux dans leurs complexes avec des molecules macrobicycliques. II. Structure cristalline et moleculaire du cryptate de baryum $C_{18}H_{36}N_2O_6{\cdot}Ba(SCN)_2{\cdot}H_2O$, Acta Cryst. 29 (1973) 1382–1387.
[22] A.N. Chekholv, Z. Neorg, Khim. 48 (2003) 1808.
[23] A.N. Chekholv, Z. Neorg, Khim. 49 (2004) 463.
[24] T. König, B. Eisenmann, H. Schäfer, Zur Reaktion von BaBiSe3 mit dem Cryptanden [2.2.2] in Ethylendiamin Darstellung und Kristallstruktur von [Ba-222Crypt] Se4·en, Z. Anorg. Allg. Chem. 498 (1983) 99–104.
[25] W.A. Wojtczak, M.J. Hampden-Smith, E.N. Duesler, Synthesis, Characterization, and Thermal Behavior of Polydentate Ligand Adducts of Barium Trifluoroacetate, Inorg. Chem. 37 (1998) 1781–1790.
[26] B.E.R. Zagler, Z. Naturforsch, B., Chem. Sci. 46 (1991) 593.
[27] D.N. Huh, J.W. Ziller, W.J. Evans, Crystal structure of the $[(THF)Cs(\mu\text{-}\eta^5{:}\eta^5\text{-}Cp')_3Yb]_n$ oligomer, Acta Cryst. 76 (2020) 1131–1135.
[28] J. Gonzalez, P. Sevilla, G. Gabarro-Riera, J. Jover, J. Echeverria, S. Fuertes, A. Arauzo, E. Bartolome, E.C. Sanudo, A Multifunctional Dysprosium-Carboxylato 2D Metall-Organic Framework, Angew. Chem. Int. Ed. 60 (2021) 12001–12006.
[29] R. Shannon, Revised effective ionic radii and systematic studies of interatomic distances in halides and chalcogenides, Acta Cryst. 32 (1976) 751–767.
[30] C. Apostolidis, G.B. Deacon, E. Dornberger, F.T. Edelmann, B. Kanellakopulos, P. MacKinnon, D. Stalke, Peter MacKinnon and Dietmar Stalke, Crystallization and X-ray structures of $[NaYb(C_5H_5)_3]$ and $Yb(C_5H_5)_2$, Chem. Commun. (11) (1997) 1047–1048, https://doi.org/10.1039/a700531h.
[31] W.J. Evans, R.A. Keyer, J.W. Ziller, Synthesis and reactivity of bis(trimethylsilyl) cyclopentadienyl samarium complexes including the X-ray crystal structure of [(Me3Si)2C5H3]3Sm, J. Organomet. Chem. 394 (1990) 87–97.
[32] C.A.P. Goodwin, N.F. Chilton, G.F. Vettese, E. Moreno Pineda, I.F. Crowe, J. W. Ziller, R.E.P. Winpenny, W.J. Evans, D.P. Mills, Physicochemical properties of near-linear lanthanide(II) bis(silylamide) complexes (Ln = Sm, Eu, Tm, Yb), Inorg. Chem. 55 (20) (2016) 10057–10067.
[33] P. Hitchcock, M. Lappert, L. Maron, A. Protchenko, Lanthanum does form stable molecular compounds in the +2 oxidation state, Angew. Chem., Int. Ed. 47 (8) (2008) 1488–1491.
[34] N.F. Chilton, C.A.P. Goodwin, D.P. Mills, R.E.P. Winpenny, The first near-linear bis (amide) f-block complex: a blueprint for a high temperature single molecule magnet, Chem. Commun. 51 (2015) 101–103.
[35] C.A.P. Goodwin, K.C. Joslin, S.J. Lockyer, A. Formanuik, G.A. Morris, F. Ortu, I. J. Vitorica-Yrezabal, D.P. Mills, Homoleptic trigonal planar lanthanide complexes stabilized by superbulky silylamide ligands, Organometallics 34 (11) (2015) 2314–2325.
[36] F. Ortu, D. Packer, J. Liu, M. Burton, A. Formanuik, D.P. Mills, Synthesis and structural characterization of lanthanum and cerium substituted cyclopentadienyl borohydride complexes, J. Organomet. Chem. 857 (2018) 45–51.